



Analytical Investigation of MHD Jeffery–Hamel flow problem with heat transfer by differential transform method

Ramakanta Meher¹  · Nirav D. Patel¹

© Springer Nature Switzerland AG 2019

Abstract

The aim of this research paper is to study and analyse the effects of Reynolds number, Hartmann number and thermal profile on velocity profiles of magneto hydro dynamics Jeffery–Hamel fluid flow between two non-parallel plates with angles 2θ and electromagnetic induction (E_0). An approximate analytical solution of the problem that is formulated using the Navier–Stokes and continuity equations has obtained in the form of a convergent series using differential transform method. The nature and the variation of the velocity profiles of Jeffery–Hamel flow with heat transfer are discussed herewith considering different thermal profiles with distinct positive values of Ha and Re in both convergent and divergent channels. The authenticity and the usefulness of this method have demonstrated by comparing with the available results of optimal homotopy perturbation method and the numerical method.

Keywords Differential transform method · Heat transfer · Jeffery–Hamel flow · System of differential equations

List of symbols

P	Pressure
k	Conductivity of the thermal
ρ	Density
T	Temperature
Re	Reynolds number
E_0	Electromagnetic induction
ν	Kinematic viscosity
M	Magnetic field
θ	Half-angle between the two plates
Ha	Hartmann number

1 Introduction

There is a great importance of incompressible fluid flow with heat transfer in cooling systems of malls and nuclear plants. The effect of angle between two unparallel walls on the velocity profiles of viscous fluid was first studied by Jeffery [8] and Hamel [6]. They derived a mathematical formulation to explain the behaviour of velocity profile

in both divergent and convergent channels. Since then, due to its importance in industry applications, some researchers analysed the Jeffery–Hamel flow problem with nano-particle with the effect of the magnetic field and heat transfer. Rivkind and Solonnikov [21] computed the solution of the stationary problem with a finite number of “outlets” to infinity in the form of infinite sectors. Akulenko et al. [1] discussed the solution of steady viscous flow in a convergent channel by taking different values of Reynolds numbers to explain the physical phenomena of the problem. Makinde and Mhone [11] used a special type of Hermite–Padé approximation semi-numerical approach to obtain the solution of the MHD Jeffery–Hamel problem, whereas the same problem was also analyzed by Esmaili et al. [4] using Adomian Decomposition Method.

Many approaches, like Travelling Wave Transformation Method, Cole–Hopf Transformation method, Optimal Homotopy Asymptotic Method, Adomian Decomposition Method, Reproducing Kernel Hilbert Space Method [16] and Generalized Boundary Element Approach were applied by several researchers to deal with

✉ Ramakanta Meher, meher_ramakanta@yahoo.com; Nirav D. Patel, nirmaths@gmail.com | ¹Department of Applied Mathematics and Humanities, S.V. National Institute of Technology, Surat, Gujarat 395007, India.



Jeffery–Hamel flow problem and other fluid mechanics problems which are inherently non-linear. Patil and Khambayat [19] used this technique for the solution of linear differential equation and later it was extended by Mirzaee [12] for finding the solution of a system of differential equation. Zhou et al. [23] applied this technique to the problems arising in electric circuit analysis. Similarly Ayaz [2] derived a solution of the system of partial differential equation using DTM whereas Chen and Ho [3] extended it to two-dimensional DTM and obtained the solution of partial differential equation. Nazari et al. [17] used it to solve a fractional order integro-differential equation with non-vocal boundary conditions. Hossein et al. [7] used Differential Transform Method and derived a solution of non-linear Gas Dynamics and Klein-Gordon equations arising in fluid flow problems. Muhmmad et al. [15] analysed the effects of magnetic fields between two parallel walls for the unsteady double phase nano-fluid flow and heat transfer using Differential Transform Method. Khudir [9] extended the Differential Transform Method to Fractional Differential Transform Method (FDTM) and solved an irrational order fractional differential equations. Kundu et al. [10] applied DTM and investigated the thermal analysis of exponential fins under sensible and latent heat transfer. Mirzaee [13, 14] extended this method to three-dimensional fuzzy Differential Transform Method and obtained the solution of fuzzy partial differential equations. Sayed and Nour [22] extended it to Modified Fractional Differential Transform Method using the Adomain Polynomials and investigated the behaviour of the projectile motion with quadratic drag force with the local path angle, velocity and position at any time t . Patel and Meher [18] used it to compute the solution of Kolmogrove–Petrovskii–Piskunov equation and also studied the behaviour of saturation profiles in fingero-Imbibition phenomena during two-phase fluid flow through porous media.

In this paper, the MHD Jeffery–Hamel fluid flow between two non-parallel plates with heat transfer is considered to analyse the effects of Reynolds number, Hartmann number and thermal profiles on velocity profiles of fluid flow. Differential Transform Method is used to study the variation of velocity profiles during MHD Jeffery Hamel flow between two non-parallel plates and thermal profiles with different values of Reynolds number and Hartmann number in both divergent and convergent channels and also checked the accuracy and the validity of the obtained results by comparing the obtained results with the results obtained by Optimal Homotopy Perturbation Method and Runge–Kutta Method.

2 Mathematical formulation of the problem

As shown in Fig. 1, consider a viscous fluid flow between two non-parallel plates with angles 2θ and (E_0) electromagnetic induction. The continuity equation, the Navier–Stokes equation and the energy equation in cylindrical coordinates can be written as

$$\frac{1}{l} \frac{\partial}{\partial l}(lu_l) + \frac{1}{l} \frac{\partial}{\partial l}(lu_\alpha) = 0 \tag{1}$$

$$u_l \frac{\partial u_l}{\partial l} + \frac{u_\alpha}{l} \frac{\partial u_l}{\partial \alpha} - \frac{u_\alpha^2}{l} = -\frac{1}{\rho} \frac{\partial P}{\partial l} + \nu \left[\frac{1}{l} \frac{\partial(l\xi_{ll})}{\partial l} + \frac{1}{l} \frac{\partial(l\xi_{l\alpha})}{\partial l} - \frac{\xi_{l\alpha}}{l} - \frac{E_0 M^2}{\rho l^2} u_l \right] \tag{2}$$

$$u_l \frac{\partial u_\alpha}{\partial l} + \frac{u_\alpha}{l} \frac{\partial u_\alpha}{\partial \alpha} - \frac{u_l u_\alpha}{l} = -\frac{1}{\rho l} \frac{\partial P}{\partial l} + \nu \left[\frac{1}{l^2} \frac{\partial(l\xi_{l\alpha})}{\partial l} + \frac{1}{l} \frac{\partial(l\xi_{\alpha\alpha})}{\partial \alpha} - \frac{\xi_{l\alpha}}{l} - \frac{E_0 M^2}{\rho l^2} u_\alpha \right] \tag{3}$$

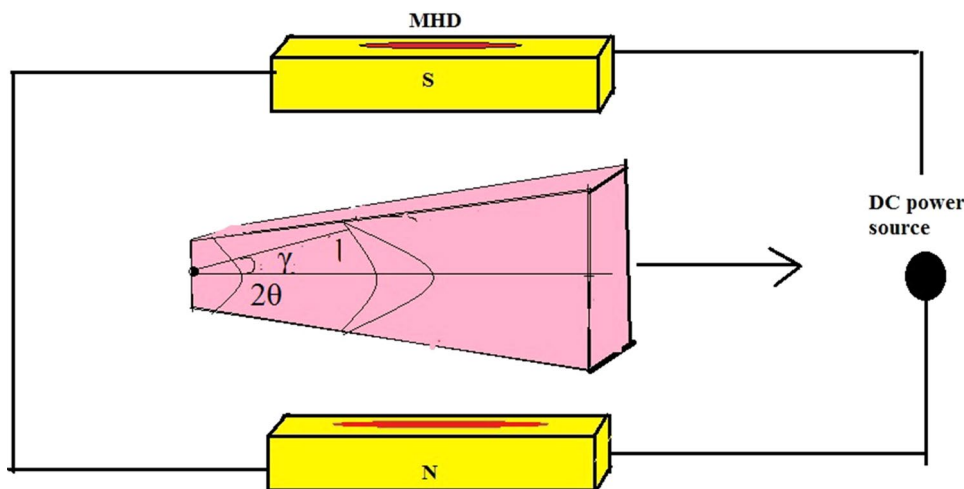


Fig. 1 3D Geometry of MHD Jeffery Hamel Flow

$$u_l \frac{\partial T}{\partial l} + \frac{k}{\rho T_p} (\nabla^2 T) + \frac{v}{T_p} \left[2 \left\{ \left(\frac{\partial u_l}{\partial l} \right)^2 + \left(\frac{u_l}{l} \right)^2 \right\} + \left(\frac{1}{l} \frac{\partial u_l}{\partial l} \right)^2 \right] + \frac{E_0 M^2}{\rho l^2} u_l^2 \tag{4}$$

where ρ is the fluid density, P is the pressure, v is the kinematic viscosity, T is the temperature, k is the thermal conductivity, T_p is the specific heat at constant pressure, E_0 is the electrical conductivity, M is the induced magnetic field and the stress components are defined as

$$\xi_{ll} = 2 \frac{\partial u_l}{\partial l} - \frac{2}{3} \text{div}(\bar{u}) \tag{5}$$

$$\xi_{\alpha\alpha} = \frac{2}{r} \frac{\partial u_\alpha}{\partial \alpha} + \frac{2 \partial u_l}{l} - \frac{2}{3} \text{div}(\bar{u}) \tag{6}$$

$$\xi_{l\alpha} = \frac{2}{r} \frac{\partial u_l}{\partial \alpha} + \frac{\partial}{\partial l} \left(\frac{2 u_\alpha}{l} \right) \tag{7}$$

Upon considering the velocity field only along the radial direction, i.e., $u_\alpha = 0$ and substituting Eqs. (5)–(7) into Eqs. (2) and (3), the continuity, Navier–Stokes and energy equations become:

$$\frac{1}{l} \frac{\partial}{\partial l} (l u_l) = 0 \tag{8}$$

$$u_l \frac{\partial u_l}{\partial l} = - \frac{1}{\rho} \frac{\partial P}{\partial l} + v \left[\nabla^2 u_l + \frac{u_l}{l^2} - \frac{E_0 M^2}{\rho l^2} u_l \right] \tag{9}$$

$$- \frac{1}{\rho l} \frac{\partial P}{\partial \alpha} + \frac{2v}{l^2} \frac{\partial u_\alpha}{\partial \alpha} = 0 \tag{10}$$

The relevant boundary conditions, due to the symmetry assumption at the channel centreline, are as follows:

$$\frac{\partial u_l}{\partial \alpha} = \frac{\partial T}{\partial \alpha} = 0, \quad u_l = \frac{u_c}{l} \alpha \quad \alpha = 0 \tag{11}$$

and at the plates making the body of the channel:

$$u_l = 0, \quad T = \frac{T_c}{l^2} \alpha^2 \quad \alpha = \theta \tag{12}$$

where u_m and T_m are the middle line rate of movement and the constant wall temperature, respectively.

From the continuity Eq. (8), one can get,

$$l u_l = g(\alpha) \tag{13}$$

$$\rho(l, \alpha) = \frac{2 \rho v}{l^2} g(\alpha) + \rho h(l) \tag{14}$$

in which $h(l)$ is an arbitrary function of l only.

Upon considering the dimensionless parameters:

$$\gamma = \frac{\alpha}{\theta}, \quad e(\gamma) = \frac{g(\alpha)}{u_m}, \quad h(\gamma) = l^2 \frac{T}{T_m} \tag{15}$$

into Eqs. (4)–(9) and eliminating the pressure term, it obtains

$$e''' + 2\theta R_e e e' + (4 - H_a) \theta^2 e' = 0 \tag{16}$$

$$h'' + 2\theta^2 h + 2\theta R_e P_r e h + \beta P_r (H_a + 4\theta^2) e^2 + \beta P_r (e')^2 = 0 \tag{17}$$

Subjected to the boundary conditions

$$e(0) = 1, \quad e'(0) = 0, \quad e(1) = 0. \tag{18}$$

$$h'(0) = 0, \quad h(1) = 0. \tag{19}$$

where $P_r = \frac{v T_p}{\rho k}$, $\beta = \frac{u_m}{T_p}$, $R_e = \frac{\theta u_m}{v}$ is the Reynolds number, $H_a^2 = \frac{E_0 M^2}{\rho v}$ is the Hartmann number and T_m is the ambient temperature.

3 Differential transform method for ordinary differential equation

Differential Transform of function $e(\eta)$ can be defined as follows:

$$E(k) = \frac{1}{k!} \left[\frac{d^k e(\eta)}{d\eta^k} \right]_{\eta=0} \tag{20}$$

where $e(\eta)$ is original function and $E(k)$ is the transformed function. The uppercase and the lowercase letters represent the transformed and the original function respectively. The inverse differential transform of $E(k)$ is defined as:

$$e(\eta) = \sum_0^\infty E(k) \eta^k \tag{21}$$

Using Eq. (20) in (21), it gives,

$$e(\eta) = \sum_0^\infty \left[\frac{d^k e(\eta)}{d\eta^k} \right]_{\eta=0} \frac{\eta^k}{k!}$$

4 Solution through differential transform method

Upon applying the fundamental operations of differential transform method to Eq. (16)–(17), it obtains,

$$(k + 1)(k + 2)(k + 3)E(k + 3) - 2qR_e \sum_{m=0}^k (m + 1)E(m + 1)E(k - m) - (4 - H_a)q^2(k + 1)E(k + 2) = 0$$

$$k + 1)(k + 2)H(k + 2) - 4q^2H(k) - 2qR_eP_r \sum_{m=0}^k H(m)E(k - m) - bP_r(H_a + 4q^2) \sum_{m=0}^k E(m)E(k - m) - bP_r(m + 1)(k - m + 1)E(m + 1)E(k - m + 1) = 0$$

And by using the conditions (18) and (19), it becomes,

$$e(\gamma) = 1 + c_1\gamma^2 + \left(-\frac{1}{6}\theta R_e c_1 + \frac{1}{12}(H_a - 4)\theta^2 c_1\right)\gamma^4 + \left(-\frac{1}{60}\theta R_e \left(2c_1^2 - \frac{2}{3}\theta R_e c_1 + \frac{1}{3}(H_a - 4)\theta^2 c_1\right) + \frac{1}{30}(H_a - 4)\theta^2 \left(-\frac{1}{6}\theta R_e c_1 + \frac{1}{12}(H_a - 4)\theta^2 c_1\right)\right)\gamma^6 + \dots$$

In particular case, for Re = 50, Pr = 1, β = 3.492161428 10⁻¹³, θ = π/24 and H = 0, we have,

$$e(\gamma) = 1 - 2.31003427572800\gamma^2 + 2.51667482980824\gamma^4 - 2.15076187988905\gamma^6 + 1.46378679137772\gamma^8 - 0.651983643033483\gamma^{10} + 0.132318469962628\gamma^{12} + \dots \tag{22}$$

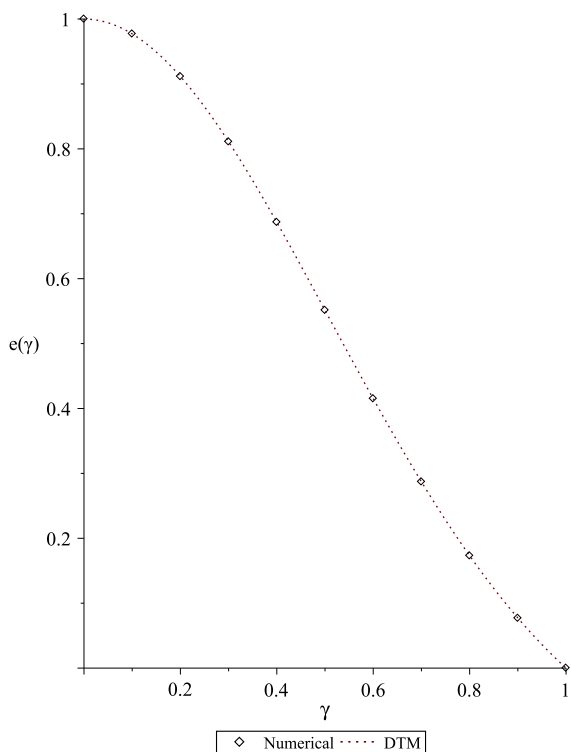


Fig. 2 Comparison between DTM and numerical results for the velocity e(γ) when H=0, θ=7.5°

$$h(\gamma) = 4.566876678 \times 10^{-13} - 3.016631685 \times 10^{-12}\gamma^2 + 3.822970788 \times 10^{-12}\gamma^4 - 3.684168116 \times 10^{-12}\gamma^6 + 3.125395871 \times 10^{-12}\gamma^8 - 2.370112507 \times 10^{-12}\gamma^{10} + 1.665857981 \times 10^{-12}\gamma^{12} + \dots \tag{23}$$

Equations (22) and (23) describes the velocity profile of Jeffery Hamel flow with heat transfer with fixed value of Reynolds and Hartmann numbers.

5 Convergence of solution

Theorem Let φ be an operator from a Hilbert space H₀ into H₀ and let E be an exact solution of Eqs. (16) and (17). Then ∑₀[∞] E(k)γ^k which is obtained by Eq. (21), converges to the exact solution, if there exists a Ψ, 0 ≤ Ψ < 1, such that ||E_{k+1}|| ≤ Ψ ||E_k||, ∀ k ∈ N ∪ {0}.

Proof We have

$$S_0 = 0, \\ S_1 = S_0 + E_1 = E_1, \\ S_2 = S_1 + E_2 = E_1 + E_2, \\ \vdots \\ S_n = S_{n-1} + E_n = E_1 + E_2 + E_3 + \dots + E_n$$

and we will show that {S_n}_{n=0}[∞] is a Cauchy sequence in a Hilbert Space H₀.

Now for ||S_{n+1} - S_n|| = ||E_{n+1}|| ≤ Ψ ||E_n|| ≤ Ψ² ||E_{n-1}|| ≤ ... ≤ Ψⁿ⁺¹ ||E₀|| for every n, m ∈ N, n ≥ m we have,

$$||S_n - S_m|| = ||(S_n - S_{n-1}) + (S_{n-1} - S_{n-2}) + \dots + (S_{m-2} - S_{m-1}) + (S_{m-1} - S_m)|| \leq ||S_n - S_{n-1}|| + ||S_{n-1} - S_{n-2}|| + \dots + ||S_{m-2} - S_{m-1}|| + ||S_{m-1} - S_m|| \leq \Psi^n ||E_0|| + \Psi^{n-1} ||E_0|| + \Psi^{n-2} ||E_0|| + \dots + \Psi^{m+2} ||E_0|| + \Psi^{m+1} ||E_0|| \leq (\Psi^{m+1} + \Psi^{m+2} + \dots) ||E_0|| = \frac{\Psi^{m+1}}{1 - \Psi} ||E_0||$$

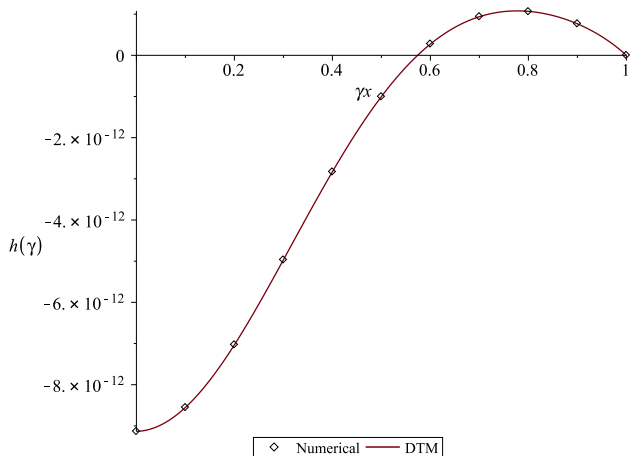


Fig. 3 Comparison between DTM and numerical results for the velocity $h(\gamma)$ when $H=0, \theta=7.5^\circ$

Which implies $\lim_{n,m \rightarrow \infty} \|S_n - S_m\|$, i.e., $\{S_n\}_{n=0}^\infty$ is a Cauchy sequence in a Hilbert space H and it convergence to S for $S \in H$.

Definition For every $i \in N \cup \{0\}$, Ψ_i can be defined as

$$\Psi_i = \begin{cases} \frac{\|E_{i+1}\|}{E_i}, & \|E_i\| \neq 0 \\ 0, & \|E_i\| = 0 \end{cases}$$

Corollary If $0 \leq \Psi_i < 1, i = 1, 2, 3, \dots$, then $\sum_{i=0}^\infty E_i$ is converges to the exact solution E .

Now by Corollary, since $\Psi_0 = \frac{\|E_1\|}{\|E_0\|} = 0 < 1, \Psi_1 = \frac{\|E_2\|}{\|E_1\|} = 0 < 1, \Psi_2 = \frac{\|E_3\|}{\|E_2\|} = 0 < 1$ similarly, $\Psi_n = 0$ for all n . Therefore $\sum_{i=0}^\infty E(k)\gamma^k$ is convergent. Similarly, $\sum_0^\infty E(k)\gamma^k$ is convergent.

6 Results and discussion

Figures 2, 3 and Tables 1, 2 discusses the comparison of the DTM results numerically as well as graphically with the existing OHPM and numerical results from which it can

Table 1 Comparison between DTM (Differential Transform Method), OHPM and Numerical solution [5] when $Ha=0$ and $\theta=7.5^\circ$ for $e(\gamma)$

γ	DTM	OHPM	NM	Error-1	Error-2
0	1	1	1	0	0
0.1	0.977149189	0.977144496	0.977142605	6.58E-06	1.89E-06
0.2	0.911491341	0.911480205	0.911479228	1.21E-05	9.78E-07
0.3	0.811006335	0.811005466	0.81100524	1.1E-06	2.25E-07
0.4	0.686905033	0.686916303	0.686914822	9.8E-06	1.48E-06
0.5	0.551291472	0.55128953	0.551288321	3.15E-06	1.21E-06
0.6	0.415134502	0.415109174	0.415108895	2.56E-05	2.79E-07
0.7	0.287100777	0.2870555	0.287054632	4.61E-05	8.68E-07
0.8	0.173268068	0.173123152	0.173122139	0.000146	1.01E-06
0.9	0.077209769	0.076872106	0.076871576	0.000338	5.3E-07
1	0.0000002	0	0	0	0

Error-1 = |DTM - NM| & Error-2 = |OHPM - NM|

Table 2 Comparison between DTM (Differential Transform Method), OHPM (Optimal Homotopy Perturbation method) and Numerical solution [5] when $Ha=0$ and $\theta=7.5^\circ$ for $e(\gamma)$

γ	DTM	OHPM	NM	Error-1	Error-2
0	-9.13E-12	-9.13456E-12	-9.1344E-12	2.00E-19	1.55E-16
0.1	-8.55E-12	-8.56173E-12	-8.554E-12	8.74E-19	7.75E-15
0.2	-7.03E-12	-7.02901E-12	-7.029E-12	1.80E-19	1.80E-23
0.3	-4.97E-12	-4.9599E-12	-4.9681E-12	2.66E-18	8.15E-15
0.4	-2.83E-12	-2.83035E-12	-2.8304E-12	1.91E-17	1.30E-23
0.5	-1.00E-12	-1.01563E-13	-1.00E-12	9.40E-17	9.02E-13
0.6	2.76E-13	2.75572E-13	2.76E-13	7.41E-18	8.00E-24
0.7	9.40E-13	9.68295E-13	9.40E-13	2.55E-18	2.85E-14
0.8	1.06E-12	1.06234E-12	1.06234E-12	2.32E-16	3.00E-24
0.9	7.68E-13	6.52409E-13	7.68E-13	6.37E-17	1.16E-13
1	0	0	0	0	0

Error-1 = |DTM - NM| & Error-2 = |OHPM - NM|

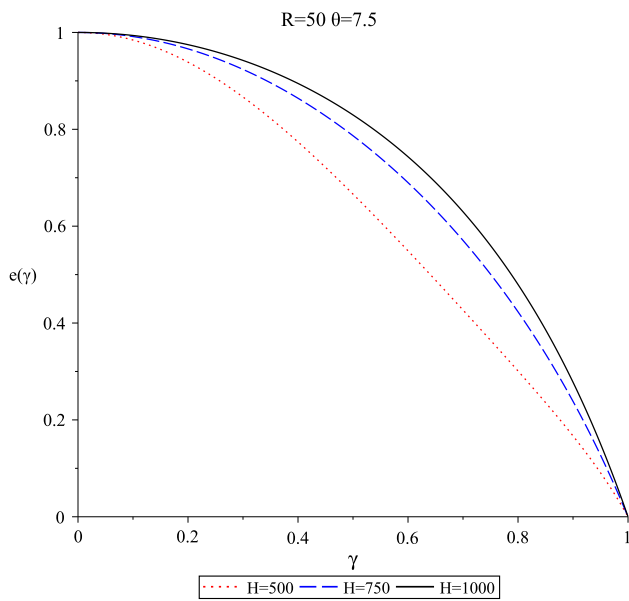


Fig. 4 Variation of velocity profiles with different Hartmann number with $\theta = 7.5^\circ$

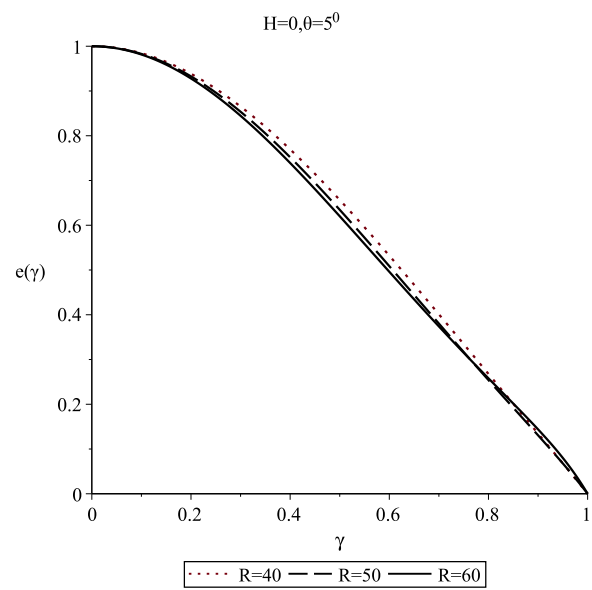


Fig. 6 Variation of velocity profiles with different Reynolds number with $\theta = 5^\circ$

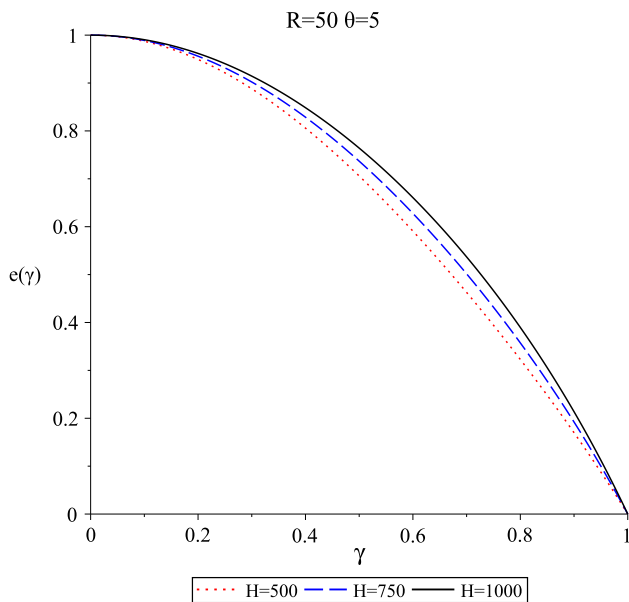


Fig. 5 Variation of velocity profiles with different Hartmann number with $\theta = 5^\circ$

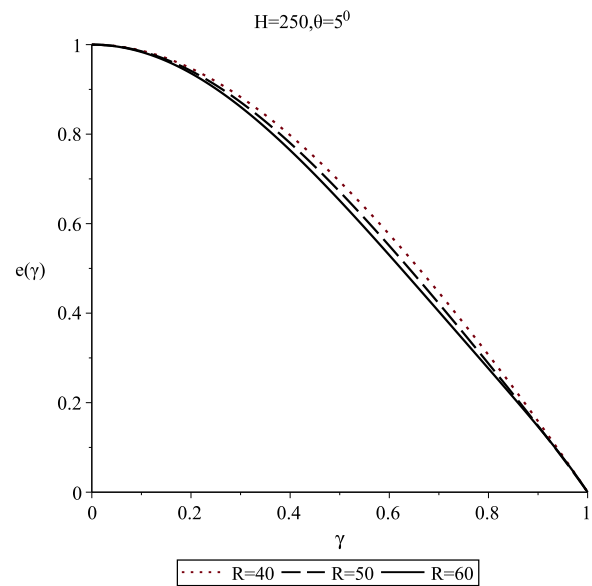


Fig. 7 Variation of velocity profiles with different Reynolds number with $\theta = 5^\circ$

be observed that there is a good agreement between the obtained DTM results with the available results.

Figures 4, 5, 6, 7, 8, 9, 10, 11 and 12 discusses the variation of velocity profiles of the MHD Jeffery Hamel flow with

the effects of different parameters. Figures 4 and 5 discuss the variation of velocity profiles for different Hartmann number keeping Re fixed, which shows that the flow velocity is increased as the value of Hartmann number increases with the fixed value of Reynolds number and it is more for

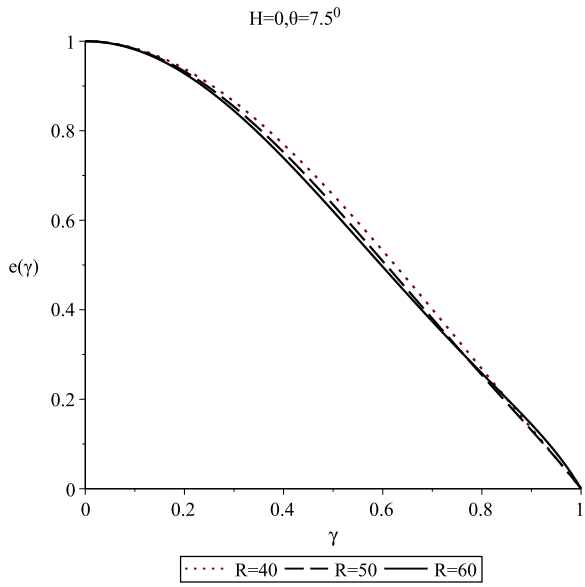


Fig. 8 Variation of velocity profiles with different Reynolds number with $\theta = 7.5^\circ$

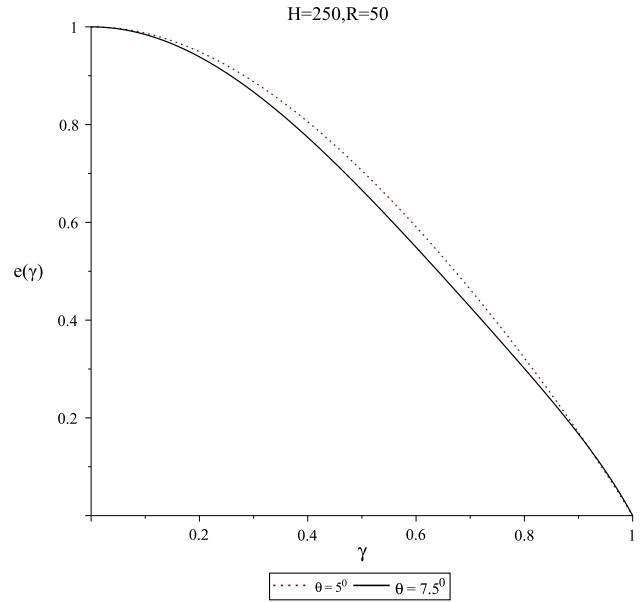


Fig. 10 Variation of velocity profiles with different angle with $H = 250$

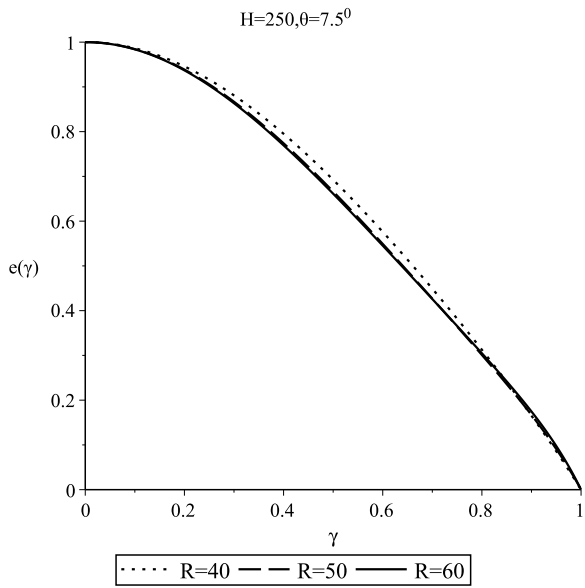


Fig. 9 Variation of velocity profiles with different Reynolds number with $\theta = 7.5^\circ$

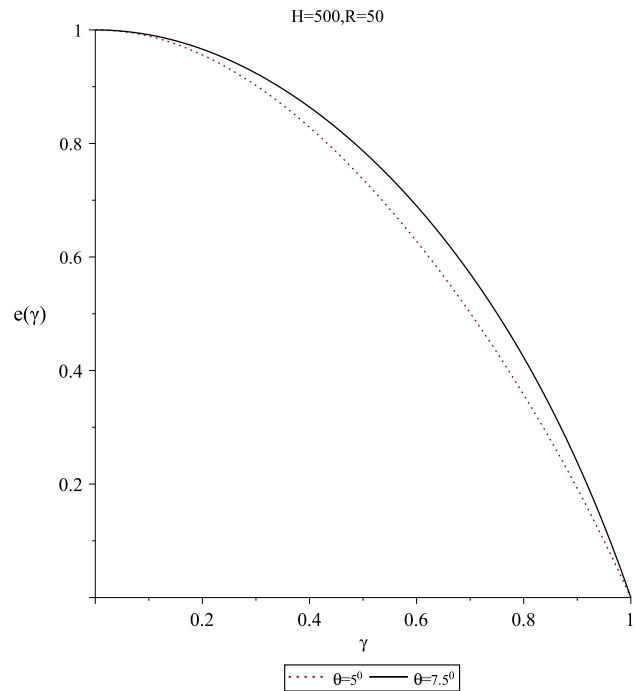


Fig. 11 Variation of velocity profiles with different angle with $H = 250$

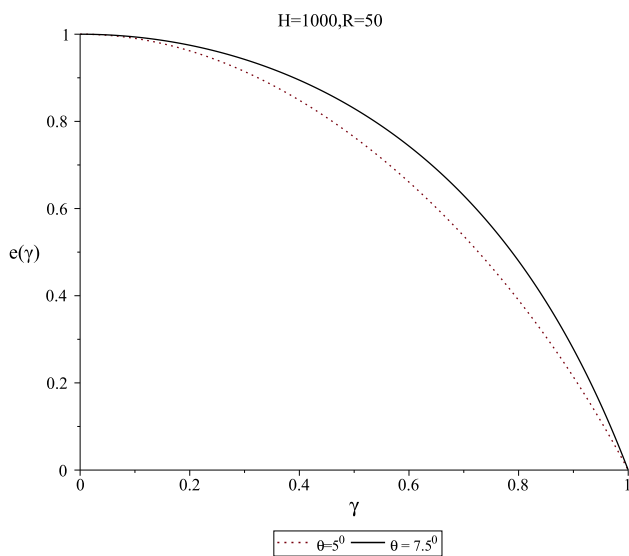


Fig. 12 Variation of velocity profiles with different angle with $H=1000$

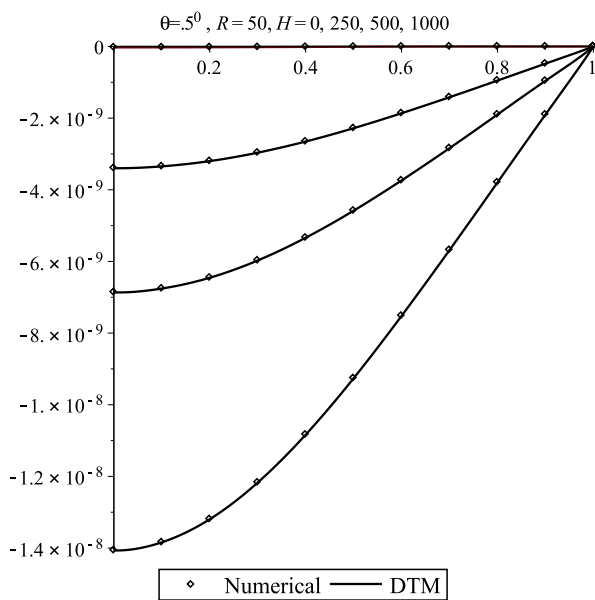


Fig. 13 Variation of thermal profiles with different Hartmann number

higher Hartmann number i.e. $H=1000$ and it is lower for $H=500$.

Similarly, Figs. 6, 7, 8 and 9 discusses the variation of velocity profiles for different Reynolds number keeping Ha

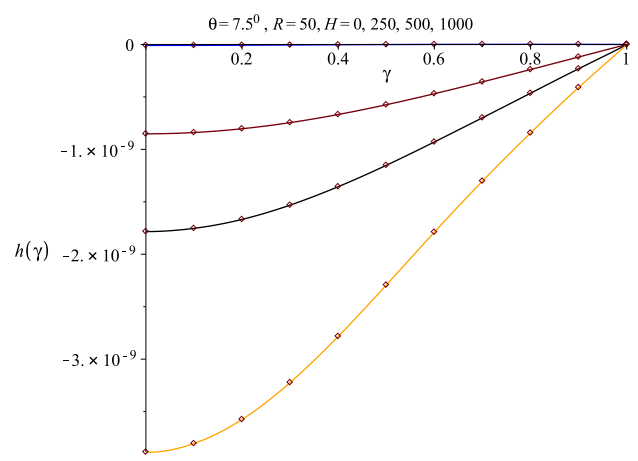


Fig. 14 Variation of thermal profiles with different Hartmann number

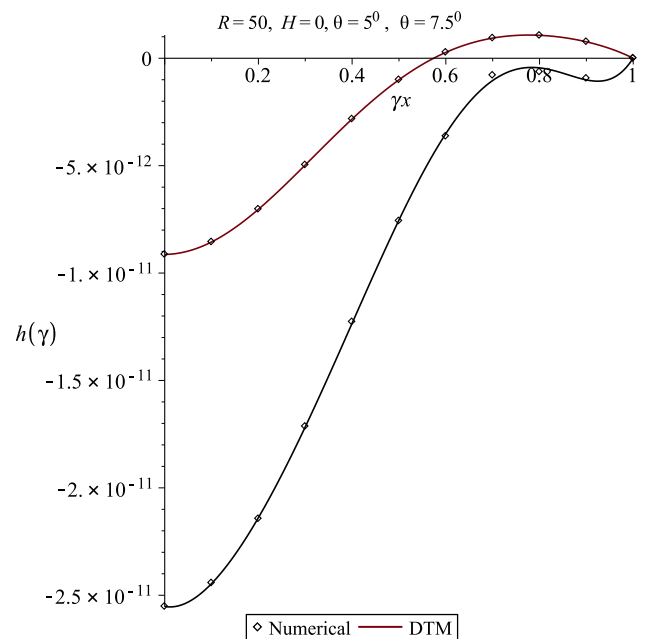


Fig. 15 Variation of thermal profiles with different angle for $H=0$

and θ fixed which shows that the flow velocity is decreased as the value of the Reynolds number is increased with the fixed value of Hartmann number and it is more for $Re=40$ while it is lower for $Re=60$.

Figures 10, 11, 12 discusses the variation of velocity profiles in divergent channels with different angles for fixed Reynolds number $Re=50$ and for different

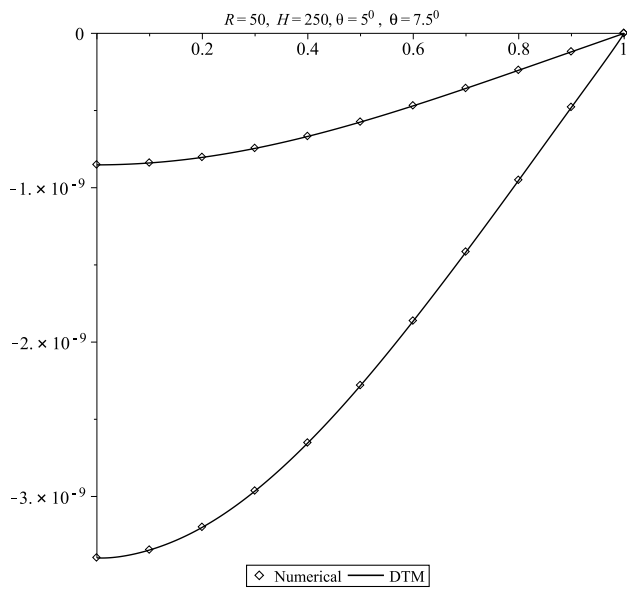


Fig. 16 Variation of thermal profiles with different angle for H=250

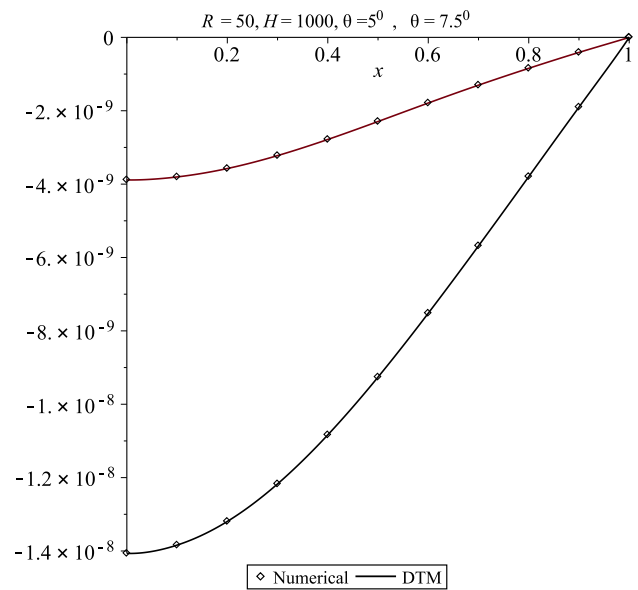


Fig. 18 Variation of thermal profiles with different angle for H=1000

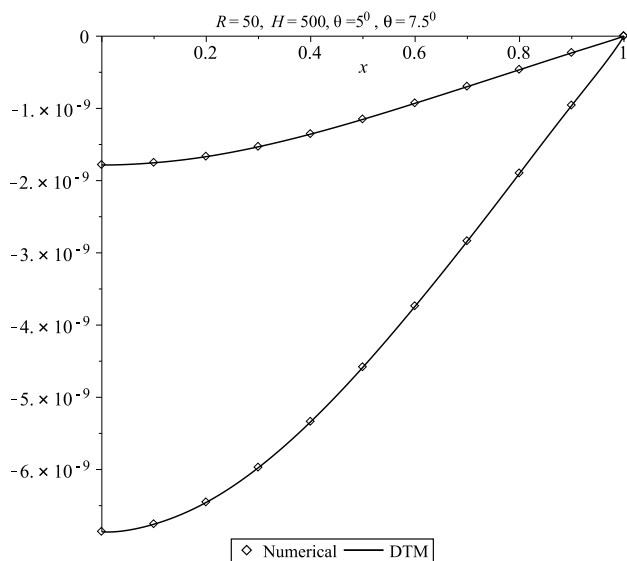


Fig. 17 Variation of thermal profiles with different angle for H=500

Hartmann number $H = 200, 500$ and 1000 which shows that the flow velocity decreases as the angel of inclination is increases and it is higher for high Hartmann

number $H = 1000$ and lower for low Hartmann number $H = 200$ keeping $Re = 50$ fixed.

The effect of Hartmann number, half angle θ and Reynolds number on the thermal profile of flow is presented in Figs. 13, 14, 15, 16, 17 and 18. From Figs. 13, 14, it can be observed that the thermal temperature decreases as the value of Hartmann number increases and it is more for higher Hartman number i.e. for $Ha = 1000$. Similarly, Figs. 15, 16, 17 and 18 discusses the effect of the half angle θ on the thermal velocity profiles which shows that the thermal temperature of the velocity profiles decreases as the angle of inclination of the plane is increases with different Hartmann number and it is maximum for $Ha = 1000$.

Tables 3 and 4 discuss the comparison of the numerical results obtained by DTM with the numerical results of Runge–Kutta method for $Re = 50$ and $\theta = 7.5^\circ$ while Tables 5 and 6 discuss the comparison of the numerical results of DTM with the numerical results of Runge–Kutta method for $Re = 50, \theta = 5^\circ$ with different Hartmann number which shows that there is a good agreement between the obtained DTM results with the available numerical results.

Table 3 Comparison of DTM with numerical solution for $Re = 50$ $\theta = 7.5^\circ$

γ	Ha = 0			Ha = 250		
	DTM	Numerical	Error	DTM	Numerical	Error
0	-9.13441E-12	-9.1344E-12	2.00E-19	-8.52003E-10	-8.52004E-10	1.123E-15
0.1	-8.55398E-12	-8.554E-12	8.74E-19	-8.39596E-10	-8.39597E-10	1.34578E-15
0.2	-7.02901E-12	-7.029E-12	1.80E-19	-8.03247E-10	-8.0325E-10	3.4678E-15
0.3	-4.96806E-12	-4.9681E-12	2.66E-18	-7.45022E-10	-7.4503E-10	8.247E-15
0.4	-2.83035E-12	-2.8304E-12	1.91E-17	-6.67641E-10	-6.67706E-10	6.48215E-14
0.5	-1.00358E-12	-1.0036E-12	9.40E-17	-5.74626E-10	-5.74674E-10	4.7798E-14
0.6	2.75572E-12	2.75572E-12	7.41E-18	-4.69072E-10	-4.69833E-10	7.60987E-13
0.7	9.39818E-12	9.39818E-12	2.55E-18	-3.56657E-10	-3.57124E-10	4.66886E-13
0.8	1.06234E-12	1.06234E-12	2.32E-16	-2.39114E-10	-2.39801E-10	6.87645E-13
0.9	7.68428E-12	7.68428E-12	6.37E-17	-1.194E-10	-1.20067E-10	6.66987E-13
1	0	0	0	0	0	0

Table 4 Comparison of DTM with numerical solution for $Re = 50$, $\theta = 7.5^\circ$

γ	Ha = 500			Ha = 1000		
	DTM	Numerical	Error	DTM	Numerical	Error
0	-1.78329E-09	-1.7833E-09	1.123E-14	-3.88589E-09	-3.8859E-09	1.123E-14
0.1	-1.753E-09	-1.75302E-09	1.34578E-14	-3.80438E-09	-3.80439E-09	1.34578E-14
0.2	-1.66678E-09	-1.66681E-09	3.4678E-14	-3.57507E-09	-3.5751E-09	3.4678E-14
0.3	-1.53128E-09	-1.53137E-09	8.247E-14	-3.22288E-09	-3.22296E-09	8.247E-14
0.4	-1.35568E-09	-1.35633E-09	6.48215E-13	-2.7829E-09	-2.78296E-09	6.48215E-14
0.5	-1.15191E-09	-1.15239E-09	4.7798E-13	-2.29317E-09	-2.29321E-09	4.7798E-14
0.6	-9.29348E-10	-9.30109E-10	0.60987E-12	-1.78929E-09	-1.79006E-09	7.60987E-13
0.7	-6.98515E-10	-6.98982E-10	4.66886E-12	-1.30247E-09	-1.30294E-09	4.66886E-13
0.8	-4.64522E-10	-4.6521E-10	6.87645E-12	-8.43574E-10	-8.44262E-10	6.87645E-13
0.9	-2.3126E-10	-2.31927E-10	6.66987E-12	-4.10076E-10	-4.10743E-10	6.66987E-13
1	0	0	0	0	0	0

Table 5 Comparison of DTM with numerical solution for $Re = 50$, $\theta = 5^\circ$

γ	Ha = 0			Ha = 250		
	DTM	Numerical	Error	DTM	Numerical	Error
0	-2.55249E-11	-2.55253E-11	3.5477E-16	-3.39773E-09	-3.39774E-09	1.523E-14
0.1	-2.44293E-11	-2.44298E-11	4.53558E-16	-3.34662E-09	-3.34664E-09	1.34568E-14
0.2	-2.14395E-11	-2.144E-11	4.64756E-16	-3.19947E-09	-3.1995E-09	3.4678E-14
0.3	-1.71427E-11	-1.71452E-11	2.42356E-15	-2.9642E-09	-2.96428E-09	8.247E-14
0.4	-1.22738E-11	-1.22773E-11	3.45558E-15	-2.65311E-09	-2.65318E-09	7.64821E-14
0.5	-7.57541E-12	-7.57905E-12	3.63636E-15	-2.28112E-09	-2.28117E-09	4.7798E-14
0.6	-3.63315E-12	-3.6367E-12	3.5477E-15	-1.86328E-09	-1.86404E-09	7.60987E-13
0.7	-7.9376E-13	-8.31636E-13	3.7876E-14	-1.4163E-09	-1.41677E-09	4.66886E-13
0.8	6.37297E-13	6.93057E-13	5.576E-14	-9.51481E-10	-9.52167E-10	6.86645E-13
0.9	9.3656E-13	9.72127E-13	3.5567E-14	-4.79194E-10	-4.79862E-10	6.67987E-13
1	0	0	0	0	0	0

Table 6 Comparison of DTM with numerical solution for $Re = 50$, $\theta = 5^\circ$

γ	Ha = 500			Ha = 1000		
	DTM	Numerical	Error	DTM	Numerical	Error
0	-6.86177E-09	-6.86178E-09	1.123E-14	-1.40649E-08	-1.4065E-08	1.123E-13
0.1	-6.75668E-09	-6.75669E-09	1.34578E-14	-1.38398E-08	-1.38399E-08	1.34578E-13
0.2	-6.45456E-09	-6.4546E-09	3.4678E-14	-1.31945E-08	-1.31948E-08	3.4678E-13
0.3	-5.97299E-09	-5.97308E-09	8.247E-14	-1.21716E-08	-1.21724E-08	8.247E-13
0.4	-5.33857E-09	-5.33864E-09	6.48215E-14	-1.08353E-08	-1.08359E-08	6.48215E-13
0.5	-4.58322E-09	-4.58327E-09	4.7798E-14	-9.25992E-09	-9.26035E-09	4.3798E-13
0.6	-3.73897E-09	-3.73973E-09	7.60987E-13	-7.51899E-09	-7.51975E-09	7.60987E-13
0.7	-2.83845E-09	-2.83892E-09	4.66886E-13	-5.68276E-09	-5.68323E-09	4.66886E-13
0.8	-1.89927E-09	-1.90615E-09	6.87645E-12	-3.79541E-09	-3.80228E-09	6.87645E-12
0.9	-9.5904E-10	-9.59707E-10	6.66987E-13	-1.90144E-09	-1.90811E-09	6.66987E-12
1	0	0	0	0	0	0

7 Conclusion

In this article, the flow behavior of the velocity profiles in MHD Jeffery–Hamel fluid flow between two unparallel plates with thermal profiles is discussed using Differential Transform Method at different slopes for different Reynolds number and Hartmann number in both convergent and divergent channels and derived the efficiency of the present method by comparing the obtained results with the available results obtained by the Optimal Homotopy Perturbation method and with the Numerical results. It can be concluded that Differential Transform Method is a reliable method that gives the solution in the form of a convergent series that can be easily handled in analysing the effect of Reynolds numbers, Hartmann numbers and half angle on both velocity profiles as well as on the heat transfer in MHD Jeffery–Hamel fluid flow.

Compliance with ethical standards

Conflict of interest The authors declare that they have no conflict of interest.

References

- Akulenko LD, Georgevskii DV, Kumakshev SA (2004) Solutions of the Jeffery–Hamel problem regularly extendable in the Reynolds number. *Fluid Dyn* 39(1):12–28
- Ayaz F (2004) Solutions of the systems of differential equations by differential transform method. *Appl Math Comput* 147:547–567
- Chen CK, Ho SH (1999) Solving partial differential equations by two dimensional differential transform method. *Appl Math Comput* 106:171–179
- Esmaili Q, Ramiar A, Alizadeh E, Ganji DD (2008) An approximation of the analytical solution of the Jeffery–Hamel flow by decomposition method. *Phys Lett* 372:3434–3439
- Fehlberg E (1982) Low-order classical Runge–Kutta formulas with stepsize control. NASA TR R-315
- Hamel G (1917) Spiralförmige bewegungen zaher flüssigkeiten. *Jahresbericht der Deutschen Mathematiker- Vereinigung* 25:34–60
- Hossein J, Maryam A, Hale T (2010) Two dimensional differential transform method for solving non-linear partial differential equations. *Int J Res Rev Appl Sci* 2(1):47–52
- Jeffery GB (1915) The two-dimensional steady motion of a viscous fluid. *Philoso Mag Ser* 6(29):455–465
- Khudiar AR, Haddad SAM, Khalaf SL (2017) Restricted fractional differential transform for solving irrational order fractional differential equations. *Chaos Solitons Fractals* 101:81–85
- Kundu B, Das R, Lee SK (2017) Differential transform method for exponential fins under sensible and latent heat transfer. *Proc Eng* 127:287–294
- Makinde OD, Mhone PY (2006) “Hermite–Padé approximation approach to MHD Jeffery–Hamel flows. *Appl Math Comput* 181:966–972
- Marinca V, Ene R (2016) Optimal homotopy perturbation method for nonlinear differential equations governing MHD Jeffery–Hamel flow with heat transfer problem. <https://doi.org/10.1515/phys-2017-0006>
- Mirzaee F, Yari MK (2016) A novel computing three dimensional differential transform method for solving fuzzy partial differential equations. *Ain Shams Eng* 7:695–708
- Mirzaee F (2011) Differential transform method for solving linear and nonlinear systems of ordinary differential equations. *Appl Math Sci* 5(70):3465–3472
- Muhammad U, Muhammad H, Khan U, Syed T, Muhammad A, Wei W (2017) Differential transform method for unsteady nano-fluid flow and heat transfer. *Alexandria Eng J* (in press)
- Mustafa I, Akgul A, Kılıçman A (2013) A new application of the reproducing kernel hilbert space method to solve MHD Jeffery–Hamel Flows Problem in Nonparallel Walls. *Abstract Appl Anal* 2013, Article ID 239454
- Nazari D, Shahmorad S (2010) Application of the fractional differential transform method to fractional-order integro-differential equations with nonlocal boundary conditions. *J Comput Appl Math* 234:883–891

18. Patel ND, Meher R (2016) Differential transformation method for solving Kolmogorov–Petrovskii–Piskunov equation and porous medium equation. *Math Sci IMRF J* 5(1):47–51
19. Patel ND, Meher R (2017) Differential transform method for solving for fingero-imbibition phenomena Arising in double phase flow through homogeneous porous media. *Math Sci IMRF J* 6(1):1–5
20. Patil N, Khambayat A (2014) Differential transform method for system of linear differential equations. *Res J Math Stat Sci* 2(3):4–6
21. Rivkind L, Solonnikov VA (2000) Jeffrey Hamel asymptotics for steady State Navier Stokes flow in domains with sector-like outlets to infinity. *J Math Fluid Mech* 2(4):324–352. <https://doi.org/10.1007/PL00000957>
22. Sayed AMA, Nour HM, Raslan WE, Shazly ES (2015) A study of projectile motion in a quadratic resistant medium via fractional differential transform method. *Appl Math Model* 39:2829–2835
23. Zhou JK (1986) Differential transformation and application for electrical circuits. Huazhong University Press, Wuhan

Publisher's Note Springer Nature remains neutral with regard to jurisdictional claims in published maps and institutional affiliations.